J. Synchrotron Rad. (1998). **5**, 639–641

Diagnostic front end for BESSY II

W. B. Peatman* and K. Holldack

BESSY GmbH, Lentzeallee 100, D-14195 Berlin, Germany. E-mail: peatman@bessy.de

(*Received 4 August 1997; accepted 17 November 1997*)

For BESSY II, synchrotron radiation beam diagnostics will be incorporated in both the insertion-device front ends and the dipole-beamline front ends. In order to gain a complete picture of the source characteristics, a diagnostic front end has been designed and tested for dipole radiation. This consists of (i) a pinhole array imaging system, (ii) a double-blade system for the determination of the vertical center of gravity of the synchrotron radiation fan, and (iii) a Bragg–Fresnel multilayer system for the most precise image information about the source size and shape.

Keywords: diagnostics; beam monitors; pinholes; blade monitors; Bragg–Fresnel optics.

1. Introduction

The behavior of high-performance beamlines at third-generation synchrotron radiation sources depends strongly on the size, position, emission angle and stability of the electron or positron beam from which the radiation emanates. A means to determine these parameters, or at least the emission angle, should be incorporated into the beamline design. In addition, all of the above parameters should be determined at one or more points in the storage ring, on-line and independently of the beamshutter position. These last two requirements are most easily fulfilled on a dipole source in the storage ring: the emission cone of an undulator beamline is too narrow and the beam time too costly for constant on-line monitoring. With these considerations in mind, a special diagnostic front end for a dipole source on BESSY II has been designed. All three systems have been built and tested at BESSY I: a pinhole array, a staggered blade pair and a Bragg–Fresnel multilayer imaging system.

2. Parameters to be measured and their size

The theoretical source parameters for the BESSY II storage ring used in this work can be found in Table 1. These assume a vertical coupling of 1%, as has been achieved at similar storage rings. The diagnostic front end is located on a 4.0° dipole source. The resolution and stability requirement for the beam are derived from the vertical source size, *i.e.* ∼41 µm/10 = 4.1 µm in the dipoles.

3. Pinhole systems

The simple principle of a pinhole camera can be employed in a monitor for the simultaneous determination of the properties of synchrotron radiation from bending magnets: source dimensions, vertical opening angle, horizontal and vertical source position and emission angle (Holldack & Peatman, 1994*a*,*b*, 1996*a*).

Table 1
Electron beam parameters for BESSY II.

$\varepsilon_x = 6 \times 10^{-9}$ m rad, $C = 001$.

Source	σ_x (µm)	σ'_x (µrad)	σ_y (µm)	σ'_y (µrad)
Straight, long	320	27	25	20
Straight, short	84	76	22	21
4.0° dipole	65	212	41	20
6.7° dipole	91	290	41	20

Table 2
Resolution and X-ray intensities from a pinhole at the detector.

Dipole source Filter material, thickness	BESSY I Al, 30 µm	BESSY II Cu, 100 µm	BESSY II Mo, 100 µm
Distance, R_1, R_2	7.1, 5.3	6.08, 2.04	6.08, 2.04
Optimum diameter, d_{opt} (µm)	63	27	20
Average filter energy, E (keV)	1.55	8.96	16.33
Filter bandwidth, E/dE (FWHM)	10	11	2.3
Image resolution, σ_i (µm)	49	16	11
Integral photon flux, I (10^8 photons s^{-1} A^{-1})	30	20	20
Vertical opening angle/at energy (mrad/keV)	0.25/1.6	0.10/9.0	0.08/1.6
FWHM at 6 m (mm)	3.4	1.4	1.1

Because of the diffraction limit, X-ray wavelengths must be used to image the source.

A single pinhole mounted at a distance R_1 from the source images an object with a magnification $M = R_2/R_1$ inversely onto the image plane at R_2. The geometrical resolution, σ_g, scales linearly with d, the pinhole diameter, while the diffraction blurring, σ_d, scales inversely with d (Hoffmann & Meot, 1982). An optimum circular pinhole diameter can be obtained when $\sigma_g = \sigma_d$, *i.e.* $d_{opt} = [1.22\lambda R_1^2/(R_1 + R_2)]^{1/2}$, leading to an image resolution of $\sigma_i = d_{opt}(R_1 + R_2)/[2(2 \ln 2)^{1/2} R_1]$.

The image produced by a pinhole with a bending-magnet source, converted on a phosphor screen to visible light, will suffer from reduced resolution if the full spectrum of the bending-magnet radiation contributes to the image. By using a filter for transmission of high photon energies, the bandwidth of the observed radiation can be made narrow and the resolution increased. For BESSY I, an aluminium filter of 30 µm thickness transmits photons of ∼1.5 keV effectively, yielding a resolution of 49 µm r.m.s. (Table 2). The aluminium filter is directly mounted on the incoming side of a phosphor screen in the vacuum system. By using a molybdenum filter on BESSY II, an image resolution of 11 µm can be achieved at photon energies of 16 keV, corresponding to $\sim\sigma_y/4$ giving semi-quantitative information on the vertical source size. For a vertical array of identical pinholes, the envelope of the individual intensities corresponds to the vertical opening angle of emission (Fig. 1). This angle can be described

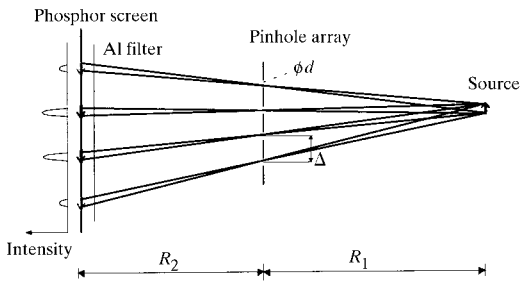

Figure 1
Geometry of a pinhole array monitor for bending-magnet radiation.

over a wide energy range by a Gaussian distribution (Table 2). The vertical spacing of the pinholes has to be larger than the vertical source size in order to avoid overlapping of the individual rays. For absolute position and emission angle measurements, both the pinhole array and a reference point in the image plane must remain fixed in space.

A two-dimensional array gives additional information about the horizontal size and intensity distribution along the dipole source. The test system incorporated a 10 (V) × 5 (H) array of pinholes of diameter 75 μm with spacings of 1 mm vertically and 2 mm horizontally, located 7 m from the source. The depth of field of each pinhole is given geometrically by the small acceptance of a pinhole looking at a horizontally curved source, here ∼18 μm. The curved path of the electrons seen by the entire array is 1.78 mm long.

The X-ray intensity pattern observed on the phosphor screen is shown in Fig. 2, a projection of one column on the right. An intrinsic scale is given by the vertical distance of 1.77 mm between the images corresponding to the magnified vertical distance, Δ, between the pinholes. The absolute position error is of the order of 100 μm, while the relative position error is less than 5 μm.

The pinholes used here were commercially laser-ablated in a 150 μm-thick tungsten sheet. An error of 10% with respect to the pinhole area can be obtained for pinholes larger than 50 μm. A thermal load of dipole magnet radiation of 3 W mrad^{-2} at 100 mA on the pinhole array in a cooled mounting frame causes a maximum temperature rise of 20 K, leading to deformations of the pinholes of only 1 μm. Recently, pinhole arrays in 100 μm of gold have been made for this project using X-ray lithography. In this case, the holes are extremely well defined and identical to ≤5% down to 10 μm diameter.

4. Staggered blade pair

For on-line measurements of the center of gravity of the vertical distribution of the radiation from dipoles, multipole wigglers and wavelength shifters, the standard two-blade detector has been extended by means of a second set of blades with the same spacing but staggered with respect to the first set (Fig. 3) (Holldack & Peatman, 1996*b*). Two such systems will be installed in the diagnostic front end in order to distinguish between source movements and changes in the angle of emission. It is the variation of this angle which causes the most problems with monochromator operation. The measurements on this system are cross checked with those from the pinhole array on the same dipole magnet.

One such system has been installed in the wavelength-shifter front end at BESSY I. Because of the large distance of the detector from the source and, in comparison, the small uncertainty of the position of the electron beam at the source point, the center of gravity measured is converted to the vertical angle of emission of the radiation.

Considering the two blades 1 and 3 in Fig. 3, one can see that the asymmetry factor of the photoemission current is determined using $A_{1/3} = (I_1 - I_3)/(I_1 + I_3)$. The asymmetry results from the spectral and angular distribution of the WLS radiation, the photoyield of the copper blades and the size of the blade opening. The main unknown parameter is the amount of radiation reflected from the blades. By employing two sets of blades, each pair with the same spacing but staggered with respect to each other, one has an internal calibration standard and, in addition, an expanded useful working range without mechanical movement. For two pairs with positions $\pm a$ mm above and below the theoretical position of the center of gravity of the radiation cone, one has the following relationships: $P = c\,A_{2/4} - a$, $P = c\,A_{1/3} + a$, $c = 2a/(A_{2/4} - A_{1/3})$, where P is the maximum of the vertical intensity distribution at the monitor and A is the measured asymmetry. These equations are valid for asymmetries between −0.5 and +0.5. By simultaneously measuring all four photocurrents, one obtains a constant value of c while the position, P, varies with the electron beam position. Because of the differing photoyields of the four blades, however, the system should be additionally calibrated by scanning it, or the electron beam, vertically in a known fashion. Space charge effects and cross talk can be avoided by biasing the blades with a negative potential. At about −100 V saturation sets in.

The measured data over several injections for the wavelength shifter at BESSY I are shown in Fig. 4. Drift of up to 50 μm corresponding to 10 μrad is observed. Variations of the emission angle as small as 0.4 μrad can be determined with an integration time constant of 1 ms. The data are continuously monitored and are coupled with steering magnets to hold the vertical position of the radiation within the working range of the beamline.

5. Bragg–Fresnel multilayer imaging system

Bragg–Fresnel multilayer (BFM) optics offer significant advantages over conventional mirror systems in that they are

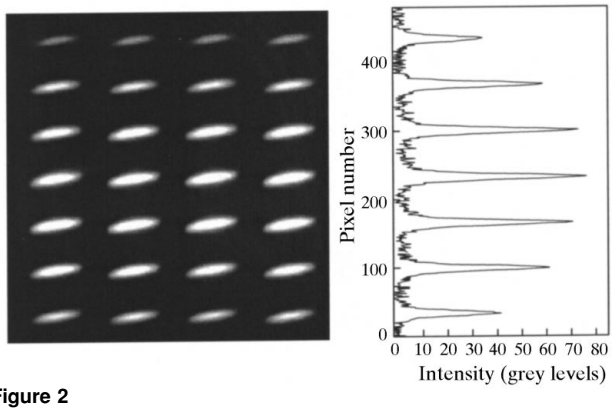

Figure 2
Left: image of a portion of the phosphor observed on a BESSY I bending magnet. Right: integrated intensities of one column of images on the phosphor.

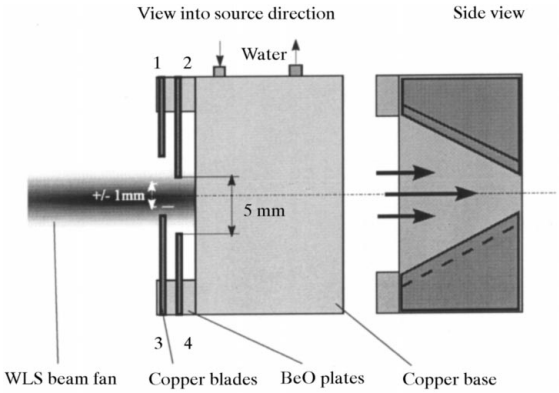

Figure 3
Layout of the staggered-blade-pair detector.

(*a*) inherently tuned to a small photon bandpass, and (*b*) can be designed to operate at high photon energies in normal incidence, thereby reducing optical aberrations (Tarasona *et al.*, 1994; Holldack *et al.*, 1995, 1996). Elliptical lenses can be readily manufactured (Erko *et al.*, 1994). They are also more suitable for the photon energies encountered on the BESSY II storage ring than crystal optics. One BFM system will be in permanent on-line operation at BESSY II in order to obtain more precise information on the shape of the radiation source in a dipole magnet than the pinhole array can deliver.

The main limitations of BFM resolution arise from the minimum zone width that can be produced, ~3 μm at the start of this development, and from optical aberrations. Both a spherical W/C lens/plane mirror system (189 eV) and an elliptical Mo/Si lens/plane mirror system (95 eV) have been manufactured (Institute of Microelectronics Technology of Russian Academy of Sciences) and tested in an $M = 0.8$ near-normal-incidence configuration at a Bragg angle of 87.2° on the BESSY I ring

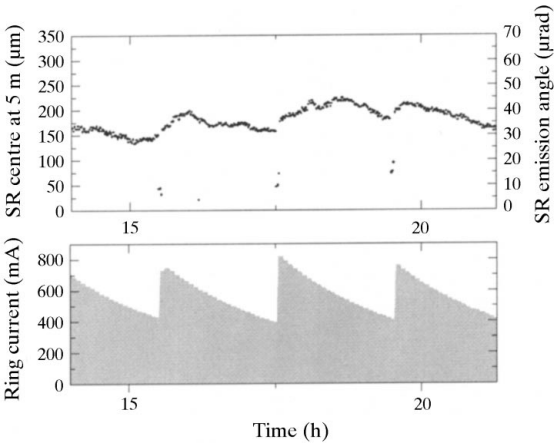

Figure 4
Behavior of the vertical emission angle of WLS radiation over several injections as determined with a staggered-blade pair at 5 m.

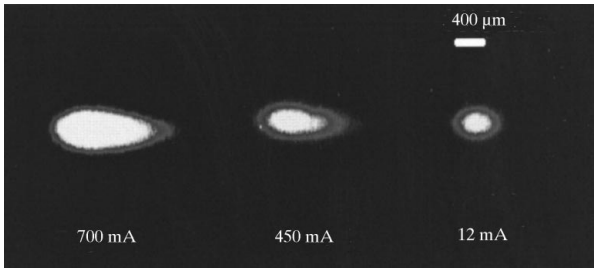

Figure 5
BESSY I source viewed with a W/C BFM lens/mirror system for three ring currents.

(Fig. 5). The Mo/Si system provides a significantly better signal-to-noise ratio and a coma-free image. The resolution of the elliptical BFM in both the vertical and the horizontal planes is given by the width of the outer zone, $1.22\Delta r_{\min} \simeq 3.6$ μm.

The rocking curve of the multilayer is relatively wide, making the acceptance aperture large and the system relatively insensitive to emission angle changes. Thus, primarily changes in the lateral position of the source are detected. The depth of focus as defined by the energy resolution of the multilayer is 6.6 cm. However, the aperture of the lens defines a smaller field depth of 1.7 mm, as given by the curvature of the electron beam in the storage ring. The demagnified image of the source on the phosphor is magnified by an objective lens on the air side of the beamline onto a 1/2″ chip of a CCD camera with 512 × 512 pixels and a 12 μm pixel size. The readout rate of the source parameters lies between 50 Hz (position only) and 5 Hz (full information).

A main disadvantage of the above system arises from the fact that, for 1:1 imaging, the detector must be as far behind the BFM lens as the lens is from the source. For BESSY II, two elliptical Bragg–Fresnel Mo/Si lenses in a normal-incidence telescope geometry with a Bragg angle of 89.3° yield a 1:1 magnification within a distance of about 12 cm behind the first lens, with the latter at a distance of 7.8 m from the source. Meanwhile, an outer-zone spacing of 1 μm can be manufactured.

6. Conclusions

All three systems described operate independently of the beamshutter and provide redundant information as a check against systematic errors. Hence, the on-line characteristics of the radiation source are always available, providing information on the health of the machine and for feedback purposes.

References

Erko, A., Agafonov, Yu., Panchenko, L. A., Yakshin, A., Chevallier, P., Dhez, P. & Legrand, F. (1994). *Opt. Commun.* **106**, 146–150.
Hoffmann, A. & Meot, F. (1982). *Nucl. Instrum. Methods*, **203**, 483–493.
Holldack, K., Erko, A., Noll, T. & Peatman, W. B. (1995). *Nucl. Instrum. Methods*, A**365**, 40–45.
Holldack, K., Erko, A. & Peatman, W. B. (1996). *Rev. Sci. Instrum.* **67**(9), 1–4.
Holldack, K. & Peatman, W. B. (1994*a*). BESSY Technical Note TN-AS 1/94, pp. 1–12. BESSY, Berlin, Germany.
Holldack, K. & Peatman, W. B. (1994*b*). BESSY Annual Report 1994, pp. 443–445. BESSY, Berlin, Germany.
Holldack, K. & Peatman, W. B. (1996*a*). BESSY Technical Note TN-AS 1/96, pp. 1–11.
Holldack, K. & Peatman, W. B. (1996*b*). BESSY Technical Report TB-AS3/96, pp. 1–6. BESSY, Berlin, Germany.
Tarasona, E., Elleaume, P., Chavanne, J., Hartmann, Ya. M., Snigiriev, A. A., Snigirieva, I. I. (1994). *Rev. Sci. Instrum.* **65**(6), 1959–1963.